

Light for Ultra Cold Molecules

Final Report for PHYS349

Friedrich Kirchner

April 28, 2006

In this final report, I will describe some of the work I did as part of my project in Kirk Madison's lab. The report will be based on my presentation for this course and will not discuss all the work I did as part of my project. In particular, work that was already discussed in my progress report, may not be discussed here.

1 Introduction

The objective of Kirk Madison and his group is to study ultra cold molecules. Laser light is involved in many parts of the experiment which is being set up at the moment. I will concentrate on the following two aspects which are related to my work.

2 Photoassociation of Li and Rb

Figure 1 schematically shows the interaction potential of a diatomic molecule. The electronic ground state (AB) and one electronically excited state (AB)* are drawn. Each electronic state can have several vibrational and rotational levels, three of which are sketched for the electronically excited state.

As a first part of their experiments, Kirk Madison and his group will measure the positions of the various rotational and vibrational levels of LiRb-molecules. They will use strong laser light to stimulate transitions from atomic states (A+B in the figure) to excited molecular levels. This process is shown on the right side of Figure 1.

In a second step of the experiment, another strong laser pulse will be used to stimulate a transition into an electronic ground state, possibly even the overall ground state of the system. This is shown on the left side of Figure 1

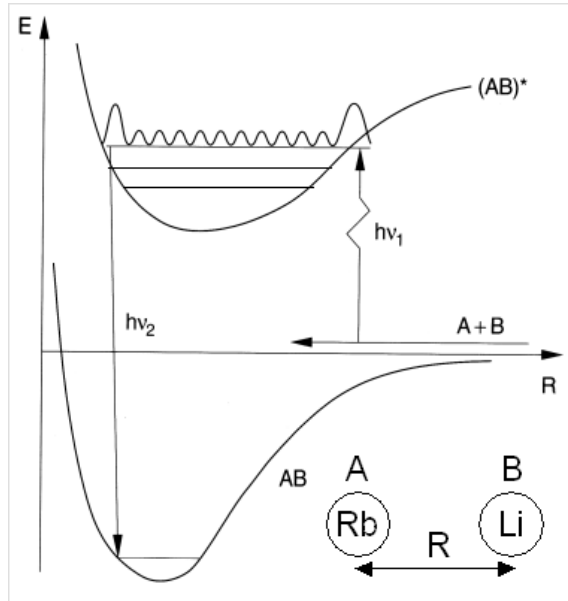


Figure 1: Schematic interaction potential of a diatomic molecule (from [3])

For these experiments, one needs a laser which is widely tunable and has a narrow linewidth which allows to measure the resonance frequencies with high precision. The Coherent 899 titanium-sapphire laser (Figure 2) is well suited for this purpose. It has a tuning range from 680 to 1100 nm and its frequency is actively controlled by an etalon pair, a piezo controlled mirror and a turnable Brewster plate. As one part of my project I assembled and aligned this laser. In the end, an output power of 2 W was reached. For details on this work please refer to my progress report.

The Coherent 899 Ti:sapphire laser will be equipped with a reference cavity which allows us to precisely stabilize (lock) the laser frequency. For completeness, I repeat the following section from my progress report.

2.1 Reference Cavity

Since we decided to copy the Coherent locking technique, we wanted the characteristics of our reference cavity to match those of Coherent's reference cavity. Fortunately, Coherent provided us with some graphs and diagrams [2] from which I was able to determine the free spectral range ν_f and the finesse \mathcal{F} of the Coherent reference cavity.

From Figure 3, I determined the free spectral range to be $\nu_f = 1$ GHz and the fringe width to be $\delta\nu_{FWHM} = 0.33$ GHz. This results in a finesse $\mathcal{F} \approx 3.17$.

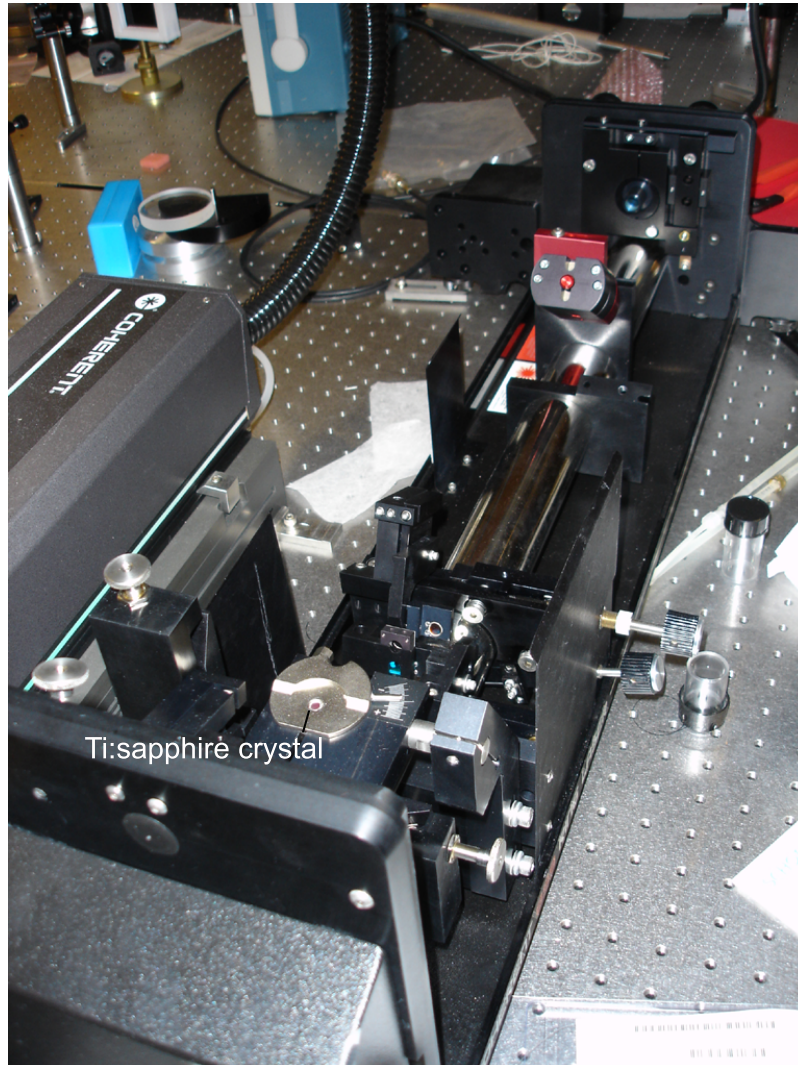


Figure 2: Coherent 899 Ti:sapphire laser, cover removed

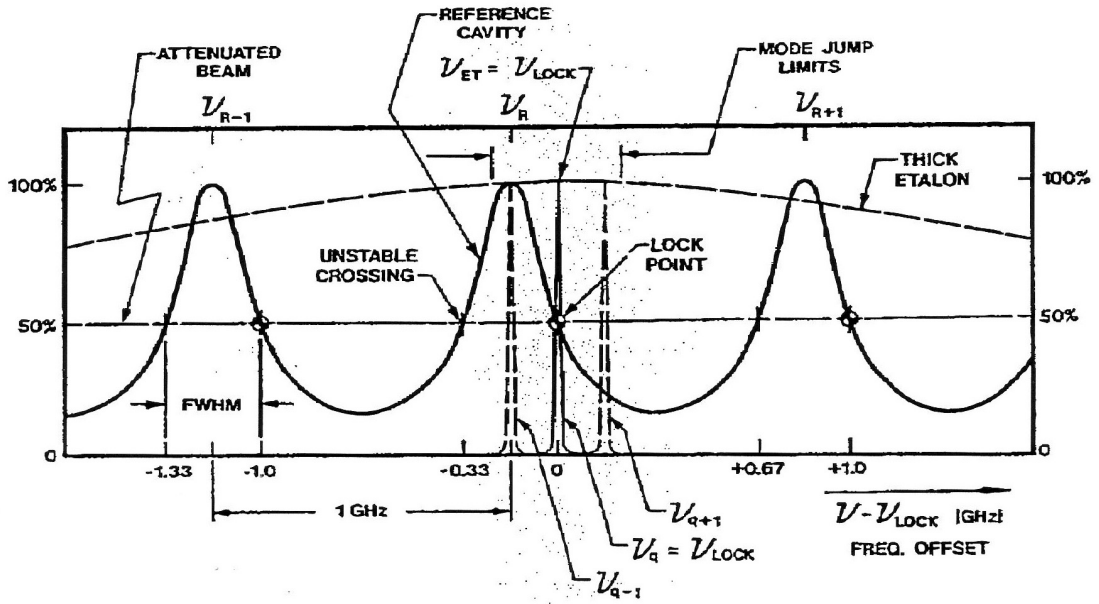


Figure 3: Coherent reference cavity: transmission (from [2])

Thus a round trip photon survival probability of $R = 14.83\%$ is required. This determines our choice of mirror reflectivity. The cavity will be a confocal setup with $R = -15$ cm spherical mirrors. A confocal resonator setup has the advantage of being less sensitive to misalignment of the incident beam, because its resonance frequencies will not change even if we do not couple in a (0,0)-mode beam.

In order to lock this cavity to an external source (i.e. a frequency comb) we will also need a galvo with a Brewster plate within the reference cavity to tune its optical path length.

I also calculated the rotation angle that would be needed for a 100 GHz scan of the cavity (assuming $\nu = 400$ THz). For a Brewster plate of 1 mm thickness, the required angle would be about 7° ($\pm 3.5^\circ$ around Brewster's angle). The effect of the turning Brewster plate on the round trip survival probability of photons is negligible. Thus, the mirror reflectivity should be $R_{Ref} = 38.5\%$.

3 Laser cooling

Ultra cold quantum gases with temperatures in the nano-Kelvin range have several interesting features that make them worth studying. Most importantly, they are a macroscopic

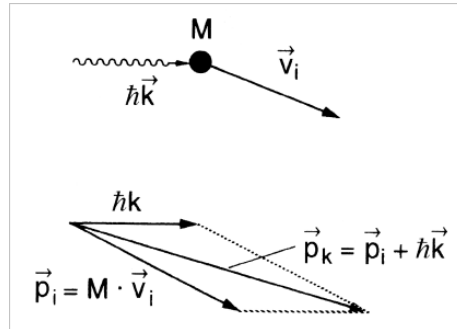


Figure 4: Atomic recoil for absorption of photon (from [3])

quantum physical phenomenon. Currently, there is a huge interest in studying these materials since one hopes to be able to test theoretical predictions in these systems. In fact, ultra cold quantum gases are expected to be the future test bench for condensed-matter theory.

Unfortunately, it is very difficult to reach temperatures in the nano-Kelvin range. In these low temperature regions, temperature is defined by the average velocity of the atoms. That is why cooling an atomic sample effectively means slowing down the atoms. In the following I will briefly discuss a technique called laser cooling.

When an atom absorbs a photon, it experiences a recoil force which is a direct consequence of momentum conservation (Figure 4). Let's assume the incident light is slightly red-tuned from the atomic resonance. In this case, due to the Doppler-shift, the light can only be absorbed by atoms traveling antiparallel to the light beam. The recoil effect then causes the atoms to lose momentum. After absorbing a photon, the atom will be in an excited state. It will return to a lower state by spontaneously emitting a photon. For this process, momentum must be conserved as well. It is important to note that the spontaneous emission is isotropic, i. e. averaged over many emission events it will not change the velocity of the atom. Therefore, one can effectively slow down atoms by shining red-detuned light at them.

This basic principle is used in a magneto-optical trap (MOT, Figure 5). It consists of six pairwise counter-propagating laser beams all of which are slightly red-detuned from the atomic resonance. In the region where all six beams overlap, optical molasses is formed in which the atoms have velocities in a small interval around $v = 0$. However, optical molasses by itself is not sufficient to spatially confine the atomic samples. This is why the MOT uses a set of magnetic coils in an anti-Helmholtz configuration. These magnetic coils produce an inhomogeneous magnetic field, which in turn causes a spatially varying Zeeman shift of the transition used for cooling. Through an adept choice of light polarizations, a position dependent radiation pressure is created which forces the atoms to the center of the MOT.

4 Absorption spectroscopy

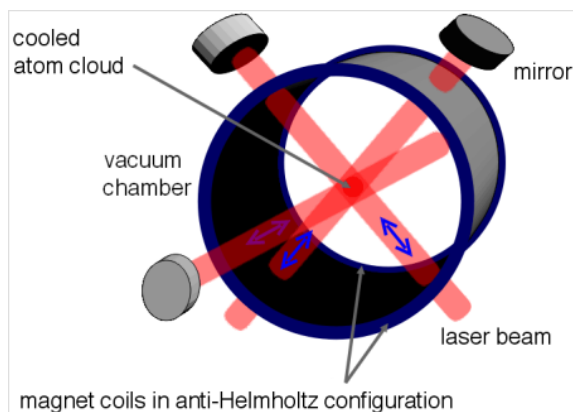


Figure 5: Magneto-optical trap

Laser cooling is limited by the fact that it uses atomic transitions with a finite (non-zero) linewidth. The minimum temperature that can be reached is given by

$$T_{min} = \hbar\gamma/2k_B,$$

where γ is the homogeneous linewidth of the atomic transition. Depending on γ , the Doppler limit can be in the range from some hundred nK to mK.

To reduce the temperature of the atomic sample even further, more sophisticated techniques are available, e. g. evaporative cooling.

In our experiment, diode lasers will be used for laser cooling purposes. Figure 6 shows a typical example of the diode lasers used in our lab. The frequency of these lasers can be tuned in a range of some nm and is controlled by the laser current, the temperature and a grating and mirror setup controlled with piezos.

To perform laser cooling, the frequency of the laser light must be precisely adjusted to the atom transition. In order to find the atomic resonance, spectroscopic measurements must be done.

4 Absorption spectroscopy

One of the standard techniques used in spectroscopy is so-called absorption spectroscopy. Its basic principle is shown in Figure 7. Laser light shines through a vapor cell, which contains the atoms one wants to study. The light that passes through the vapor cell is measured in a photo detector. When the laser light is at a resonance frequency of the atomic sample, it will be absorbed in the vapor cell. Otherwise, the light will simply pass

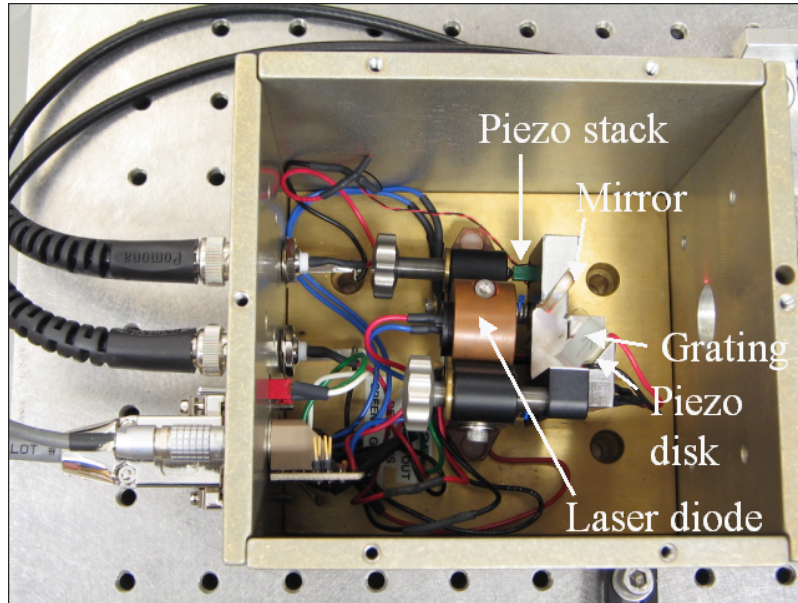


Figure 6: Diode laser

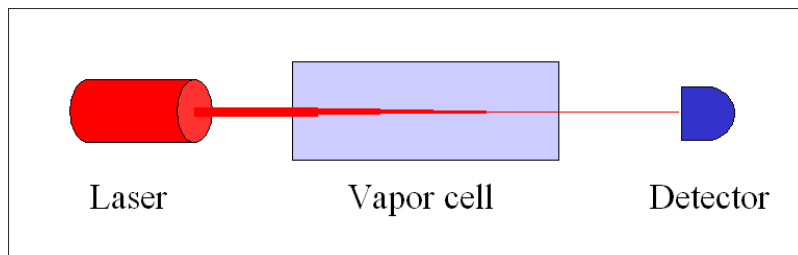


Figure 7: Schematic of an absorption spectroscopy experiment

through the cell. By sweeping the frequency of the laser light, one can obtain the spectrum of the atoms.

Figure 8 shows the Lithium D1 and D2 lines (green data points). The voltage sweep (black) and the transmission signal from a Fabry-Perot cavity (red) are shown for reference. Figure 9 shows the energy levels for Lithium. Comparing these energy levels to the measured data one finds a nice agreement in the spacing of the D1 and D2 lines. However, the hyper-structure splittings cannot be resolved. Note however, that we cannot expect to see the effects of the hyper-fine splittings of the top two levels since their splitting is on the order of the natural linewidth (approx. 10 MHz) of the transition. However, the hyper-fine splitting of the lowest level should be detectable and we would expect both the D1 and the D2 line to be split in two separate lines.

4 Absorption spectroscopy

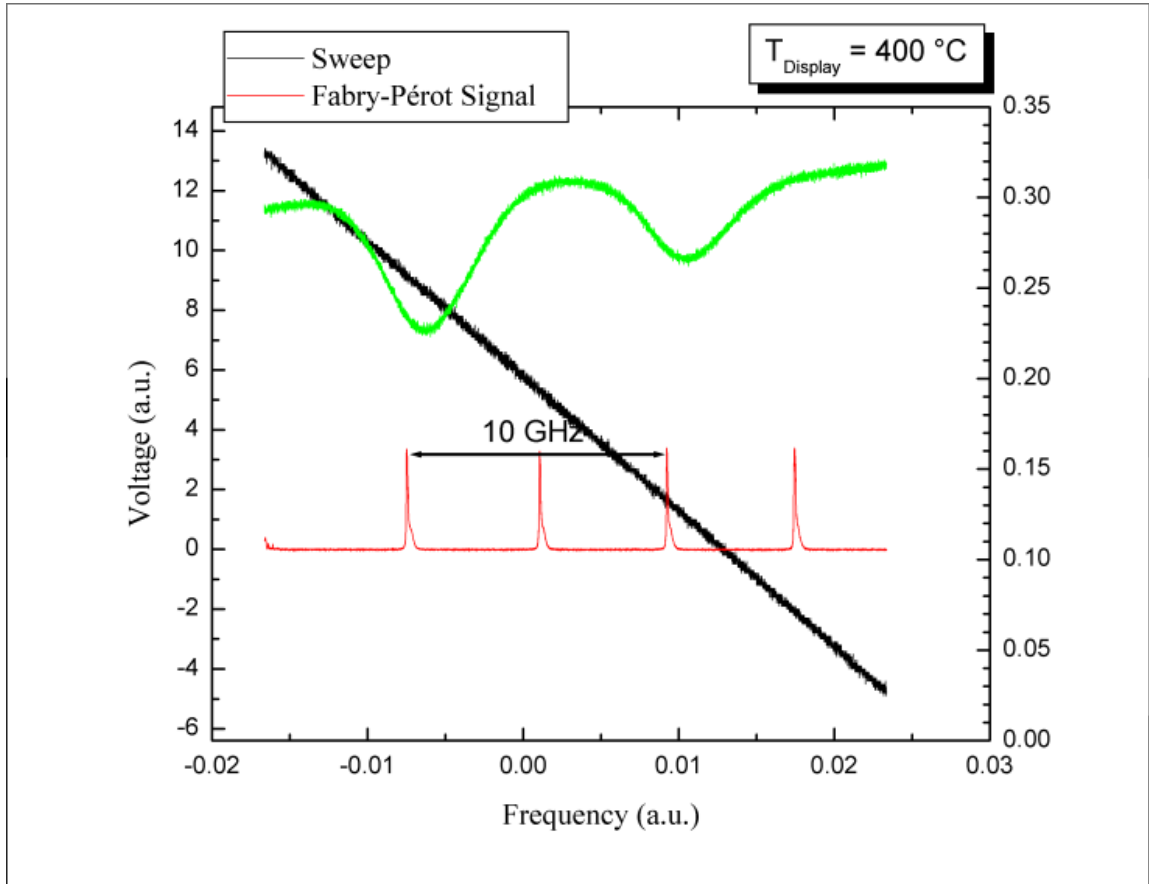


Figure 8: Absorption spectrum of Li

4 Absorption spectroscopy

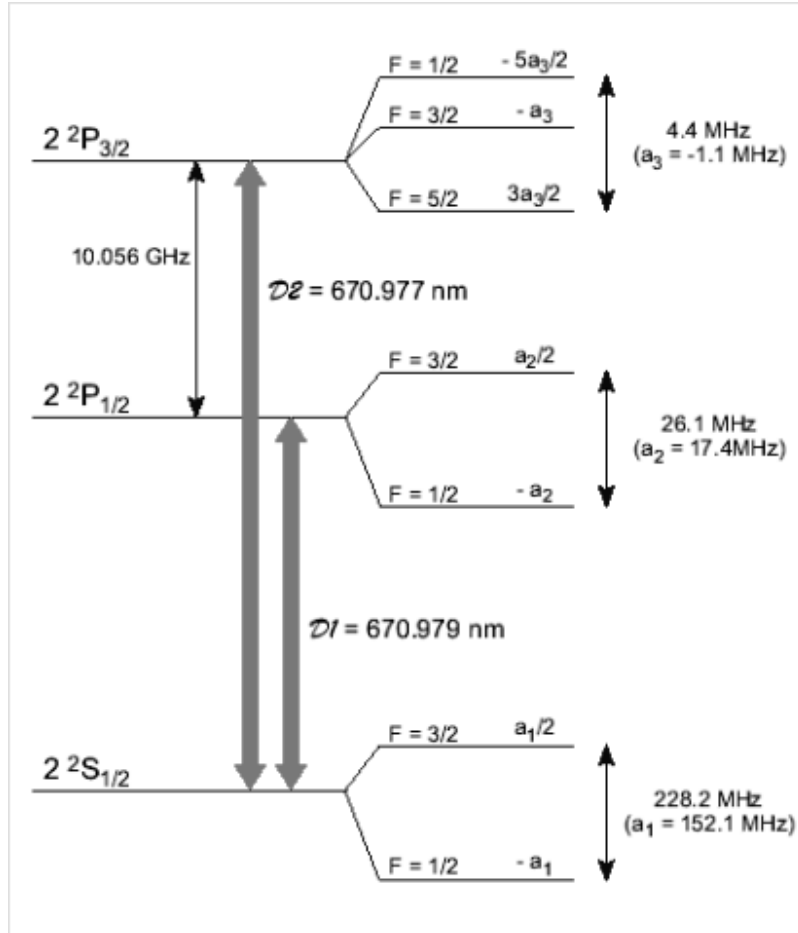


Figure 9: Energy levels of Li

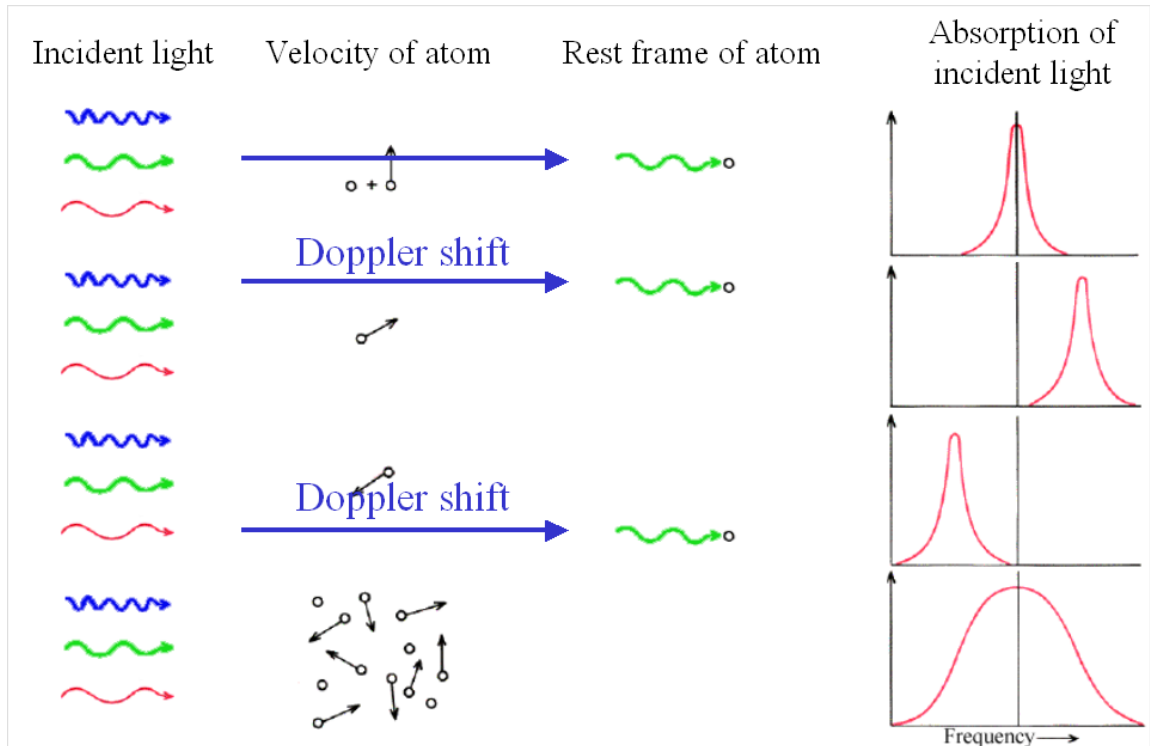


Figure 10: Doppler broadening (schematic) (from [1])

The reason why we are unable to detect the hyper-fine splitting is so-called Doppler broadening. It is shown schematically in Figure 10. It is caused by the thermal movement of the atoms.

Atoms at rest or with no velocity component parallel to the direction of the incident light will absorb light at their atomic resonance frequency. However, atoms that have a velocity component parallel to the direction of the light will absorb light which is slightly off the atomic resonance frequency. This is because of the Doppler effect which causes the frequency shift between the frequency in the lab frame and the one that the moving atom sees in its own rest frame.

Since the thermal gas in the vapor cell contains atoms traveling at many different velocities, the spectrum will be broadened and the natural linewidth of the atomic transition will be obscured.

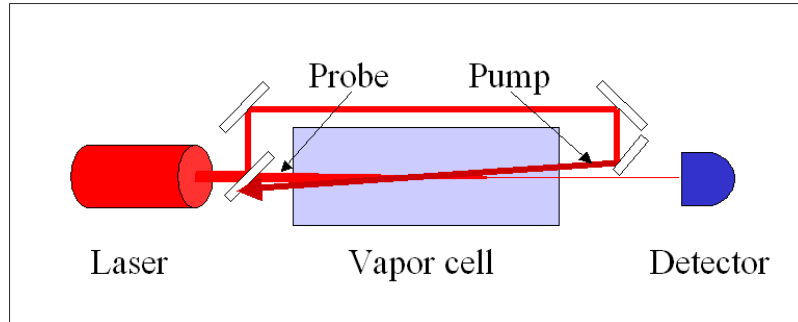


Figure 11: Schematic of a saturated absorption spectroscopy experiment

5 Saturated absorption spectroscopy

The problem of Doppler broadening can be overcome with a technique called saturated absorption spectroscopy. Its schematic is shown in Figure 11. In addition to a weak probe beam that shines through the vapor cell and onto a detector, a strong pump beam counterpropagates through the cell and overlaps with the probe beam.

Figure 12 shows the saturated absorption experiment I set up for Lithium. Pump and probe beam are traced for clarity.

The fundamental principle of saturated absorption spectroscopy is depicted in Figure 13, which assumes a two-level atom. First, let's assume the incident light is off the atomic resonance frequency. Since the pump and the probe beam travel through the vapor cell in opposite directions they will be absorbed by different sets of atoms. This is due to the Doppler-shift as described above.

However, when the pump and the probe beam are on the atomic resonance frequency, they interact with the same set of atoms, atoms with no velocity component along the light direction. When no light at the transition frequency is present, the upper and the lower level of the (two-level) atom will be occupied according to the Boltzmann distribution. This means the upper level is almost completely unoccupied because its energy lies about 1 eV (an optical photon) above the ground state. In the presence of the strong pump light, the transition will be saturated, which means that upper and lower level are equally populated. Accordingly, the lower level is occupied much less than before. This is why the (weak) probe light will be absorbed less.

Since real atoms are not two-level systems, the situation is slightly more complicated. Assume for example, that there are two closely spaced spectral lines with frequencies ω_a and ω_b and a common lower state. If we shine light at the central frequency $\frac{1}{2}(\omega_a + \omega_b)$ at the atoms, the pump beam will excite both transitions. Let's assume transition ω_a is excited in atoms traveling parallel to the pump beam, transition ω_b is excited in atoms traveling

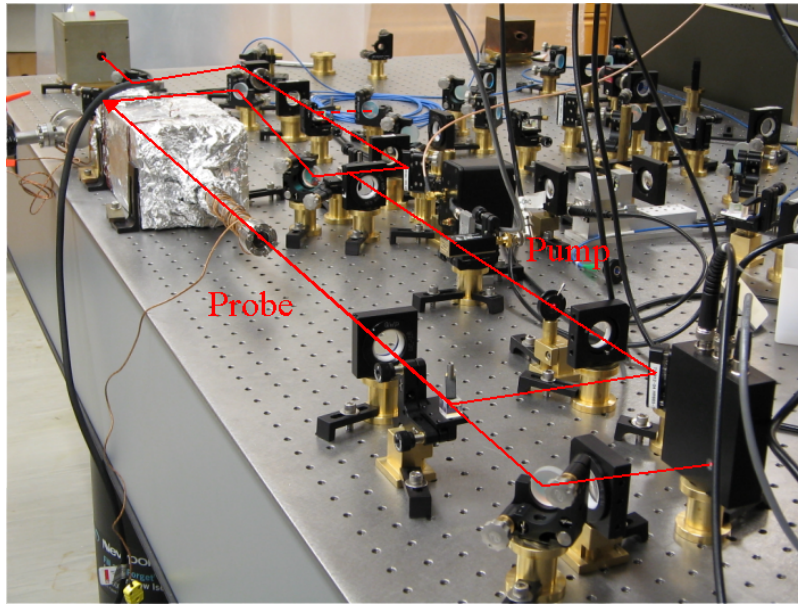


Figure 12: Experimental setup of saturated absorption experiment in Li

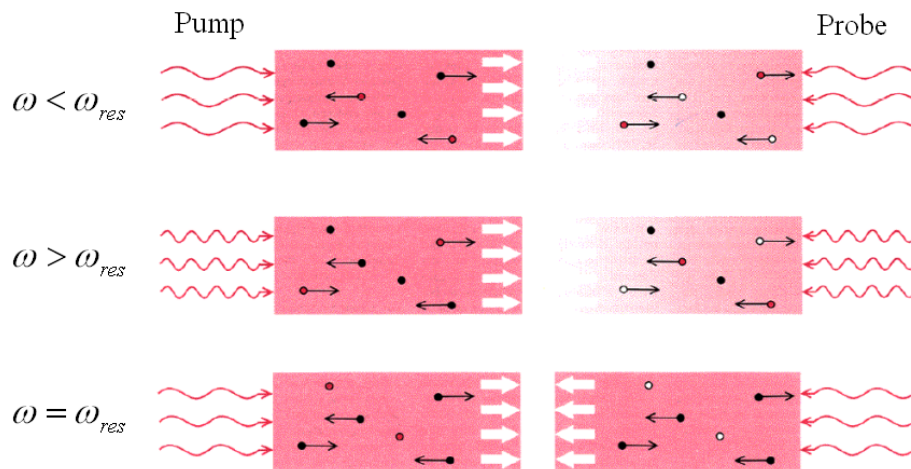


Figure 13: Saturated absorption spectroscopy (schematic), red dots depict atoms which are being excited by the incident light, white dots depict atoms which have been excited by the pump and are no longer available to absorb probe light (from [1])

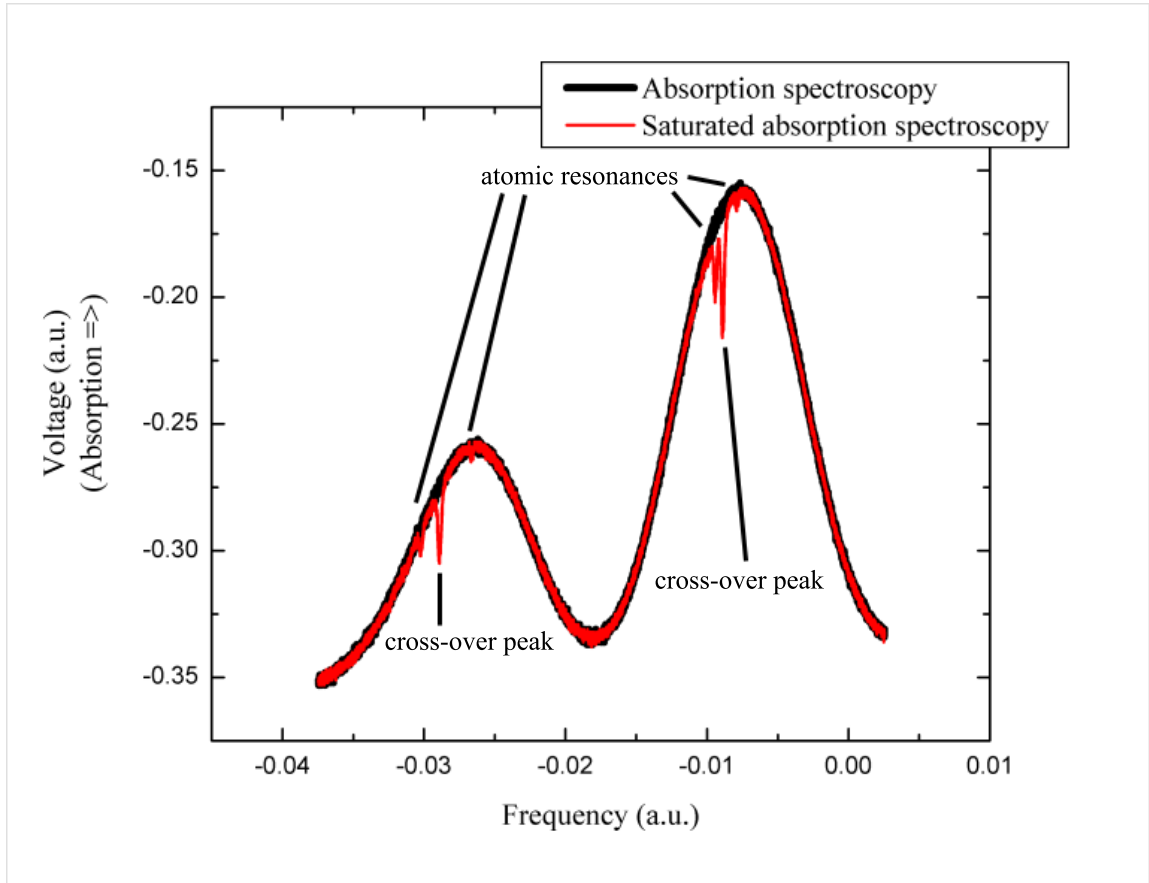


Figure 14: Experimental results of absorption spectroscopy and saturated absorption spectroscopy in Rb

antiparallel to the pump beam. The probe also interacts with both these sets of atoms (although it is absorbed in different transitions). However, due to the effect of the pump beam, the lower state of the atoms is populated less, which results in a reduced absorption of the probe light. These pseudo-resonances are called cross-over resonances.

In conclusion, what we expect to find is the following: Away from the resonance frequency of the atomic transition we expect to see the same Doppler-broadened spectrum as in regular absorption spectroscopy. However, there will be reduced absorption when we hit an atomic resonance frequency. In addition, cross-over peaks may appear between two closely spaced spectral lines. This is exactly what we see in Figure 14.

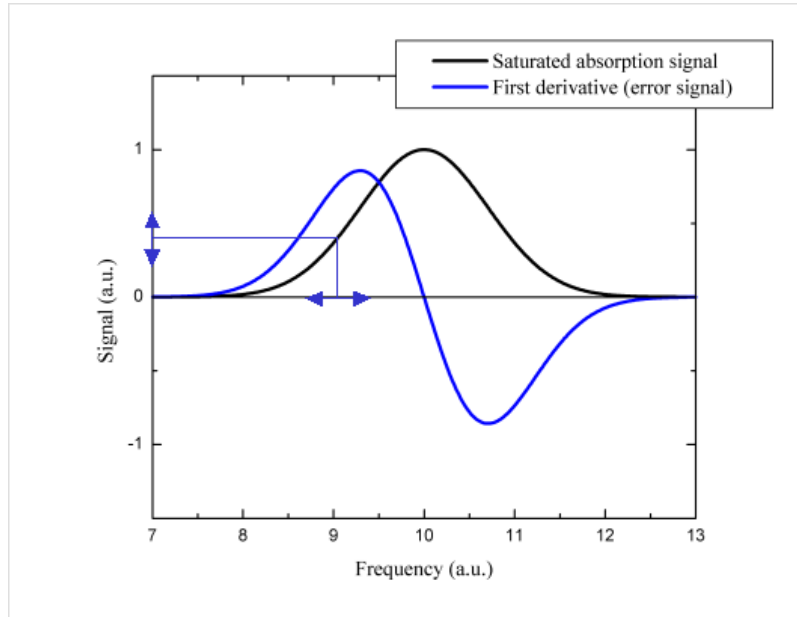


Figure 15: Creation of an error signal (schematic)

6 Locking of diode lasers

The signal we get from the saturated absorption experiment has a significantly smaller linewidth than the Doppler-broadened signal. It is therefore suitable to use this signal to lock our laser. This means that we want to actively stabilize the frequency of the diode laser to one of the Lithium transition frequencies. To do so, we would like to obtain an error signal which is positive on one side of the resonance and negative on the other side. This error signal can then be used to compensate drifts in the laser frequency.

Obviously the absorption signal itself is not a good candidate for an error signal because it shows the same behavior on both sides of the atomic resonance. However, the first derivative of the absorption signal is more suitable and has the desired properties. This is illustrated in Figure 15.

The first derivative of the absorption signal can be obtained from the experiment when so-called lock-in detection is used. This technique also has the advantage of dramatically improving the signal-to-noise ratio of the signal.

To use this technique we have to modulate the light frequency $\nu = \nu_0 + \delta\nu \cdot \sin \omega t$ by a small amount $\delta\nu$. Consequently, the signal will also be modulated and can be expanded

around ν_0 .

$$S(\nu) = S(\nu_0) + \left. \frac{dS}{d\nu} \right|_{\nu_0} (\delta\nu \cdot \sin \omega t) + \left. \frac{d^2S}{d\nu^2} \right|_{\nu_0} (\delta\nu \cdot \sin \omega t)^2 + O(\delta\nu^3)$$

In a phase-sensitive amplifier, the signal is multiplied by a sine function with the same modulation frequency and then time-averaged. The output signal depends on the phase φ of the multiplied sine function. This phase can be used to compensate for a phase difference between the signal from the experiment and the reference sine function which the signal is multiplied with. In the experiment it is normally chosen so that the greatest output signal is achieved.

$$\frac{1}{T} \int_0^T \sin(\omega t + \varphi) S(\nu) dt \propto \left. \frac{dS}{d\nu} \right|_{\nu_0} \delta\nu + O(\delta\nu^3)$$

What results is an output signal proportional to the first derivative of the absorption signal plus some terms of higher order in the modulation amplitude.

Using this kind of setup, I was able to lock lasers to the resonance frequencies of both Li and Rb.

References

- [1] T. W. Hänsch, A. L. Schawlow, G. W. Series: *Das Spektrum des atomaren Wasserstoffs*, Spektrum Verlag
- [2] Coherent: *Figure 1.1-24. Reference Cavity: Transmission*, facsimile
- [3] W. Demtröder: *Laser Spectroscopy*, Springer (2003)

Appendix: Progress report

On the following pages my progress report can be found.

Progress Report for PHYS349

Assembly and Upgrade of a Coherent 899-01 Ti:Sapphire Laser

Friedrich Kirchner

December 20, 2005

1 Introduction

The objective of this project is to assemble and upgrade a Coherent 899-01 Ti:Sapphire laser, which is shown in Figure 1. This laser will eventually be locked to a high precision frequency comb and thus provide a frequency standard for molecular photoassociation spectroscopy on rubidium and lithium atomic gasses.

I work on this project together with Keith Ladouceur, a master's student in Kirk Madison's lab.

2 Setup of Coherent 899-01 Laser

Setting up the original laser turned out to be more complicated than expected. The way we first placed the laser on the optics table was such that the pump laser beam from a 10 W Coherent Verdi diode laser had to travel about 2 meters before entering the 899 laser. We tried to align the elements of the 899 laser as described in the manual of the laser but could not achieve lasing.

Since Coherent recommends a distance between the pump laser and the 899 laser of about half a meter and because we realized that we did not have enough space behind the laser to feed the emitted beam into an optical fibre, we decided to change the position of the laser.

Previously, we had used a removable mirror to direct the beam to our experiment, but since the alignment precision was so critical we decided to use a fixed setup. This was realized with a turnable half-wave-plate and a polarization beam splitter. Depending on

2 Setup of Coherent 899-01 Laser

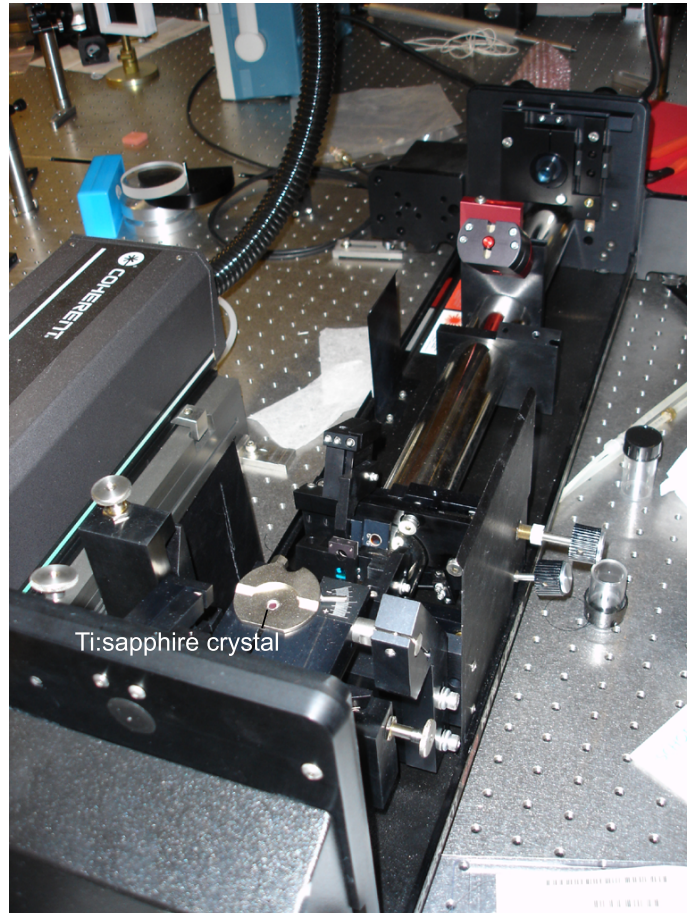


Figure 1: Coherent 899 Ti:sapphire laser, cover taken off

the position of the half-wave-plate, light was directed to our setup or was available for other experiments.

We restarted the alignment process which involved removing several optical components from the setup. Those had to be reinserted during the alignment. The alignment required high precision work and the apparatus was not very forgiving. That is why we needed a lot of time as well as help from Valery Milner (who had worked with this kind of laser before) to achieve lasing action. However, even at 10 W pumping power an output of only a few hundred mW was achieved.

The next step was to fine-tune the alignment of the different elements of the laser. Within the ring cavity of the laser, there are four mirrors which can be tilted in horizontal and vertical direction. Finding the ideal positions of those four mirrors was tedious and involved a technique called “walking the beam” which is described in the following paragraph.

First, move the mirror closest to the pump so that the setup is still lasing but at a lower intensity. Then try to adjust the mirrors of the ring cavity to achieve maximum output. If the maximum output is less than before, undo the change on the first mirror (restore the original setting) and change it in the opposite direction. Otherwise, continue in the same direction as before. By doing so, Keith achieved an output of more than 2 W at a pump power of 10 W.

3 Upgrade

In the current setup the 899 laser operates as a broadband laser. However, for its intended use we need a single-frequency laser which can be actively stabilized to a reference frequency.

The Coherent intra-cavity etalon assembly (ICA) is a setup of two etalons, which can be controlled electronically. Together with a piezo driven tweeter mirror and a galvo driven Brewster plate, these etalons will be used to actively control the resonance frequency of the ring cavity.

When I started working on this project it was unclear, how the upgrade of the broadband laser to a single-frequency laser would be realized. Various options were considered, including the purchase of an upgrade from Coherent and our own construction of all the necessary parts. We finally decided to get some parts from Coherent and to construct other parts ourselves.

3.1 ICA Mount

Since we already own the ICA we need to obtain a mount in order to fix the ICA within the laser assembly. Since a neighboring lab uses this part in one of their lasers, we had the chance to look at the device, measure its dimensions and take pictures. On the basis of this data, I was able to design the part using the CAD software IronCAD.

Since I had never used this software before, I needed some practicing time before I could successfully complete the design of the ICA mount. As well, my unfamiliarity with North American measuring units caused some difficulties. Having measured the dimensions of the original parts in millimeters, the measurements were mostly really odd numbers. However, this changed when I converted the values into inches.

Figure ?? shows the complete assembly of the ICA mount. Figure 3 shows design details of the central piece which is connected to the ICA. This part allows two dimensional movement of the ICA by means of four setscrews.

The drawings were submitted to a local machining company for a quote. This quote was only slightly less expensive than the original part from Coherent. That is why we decided not to have the ICA mount machined but to get the original part.

3.2 Other Components

Other components needed for the upgrade include the piezo tweeter mirror and the galvo turning a Brewster plate. We looked into constructing these parts ourselves but eventually decided to buy them, mainly because the mounts for those parts would be complicated to make, especially since we do not know the exact dimensions.

Another key component of the laser upgrade is the electronic circuitry controlling the various parts of the laser (ICA, tweeter mirror, galvo). Without specific information from Coherent about the voltages and currents that are needed to drive the various parts, it would have been very difficult (if not impossible) to design the control circuitry. As well, we had to consider how long it would take to get part built once we had designed them. Overall, it made more sense to purchase the control electronics from Coherent which we decided to do.

3.3 Locking Mechanisms

Our original plan was to use the locking scheme developed by Hänsch and Couillaud to lock our laser to a stabilized reference cavity. This is why I familiarized myself in detail with this technique which will be discussed in the following section.

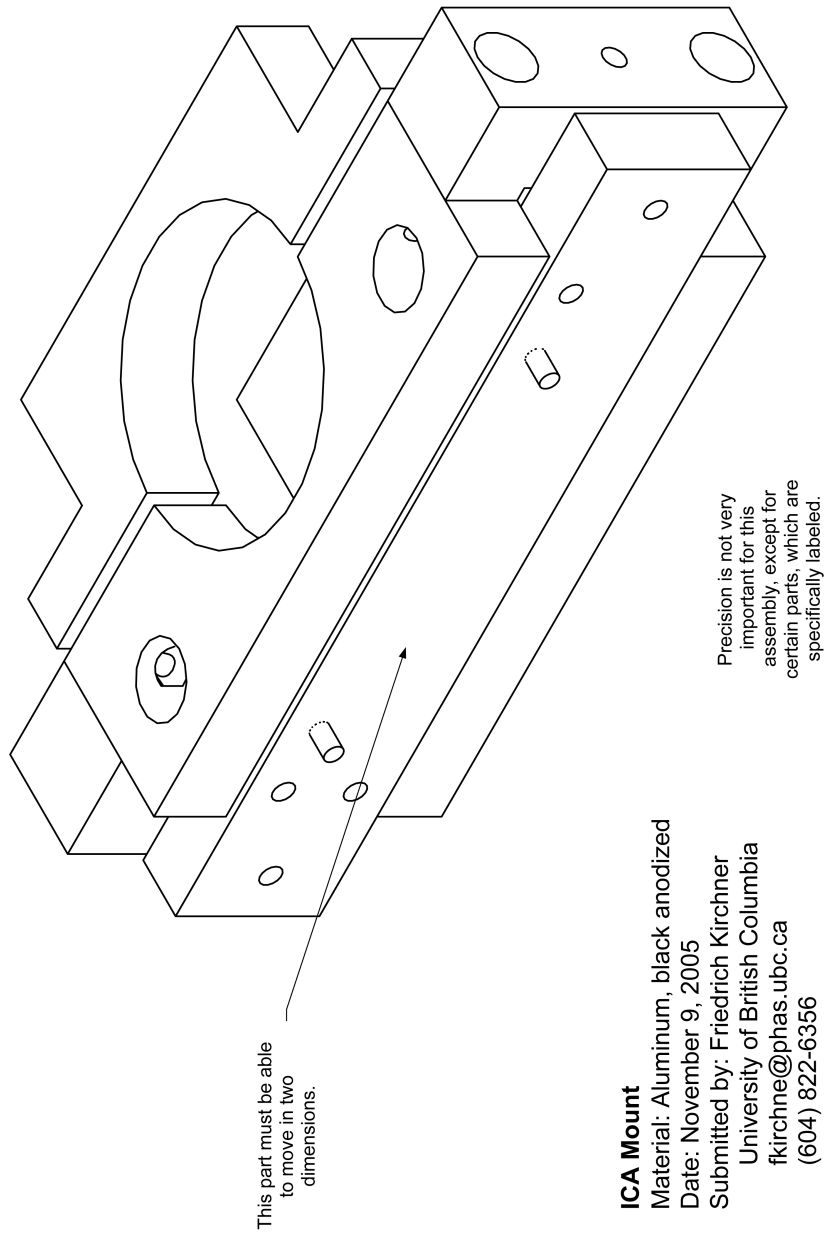


Figure 2: ICA mount

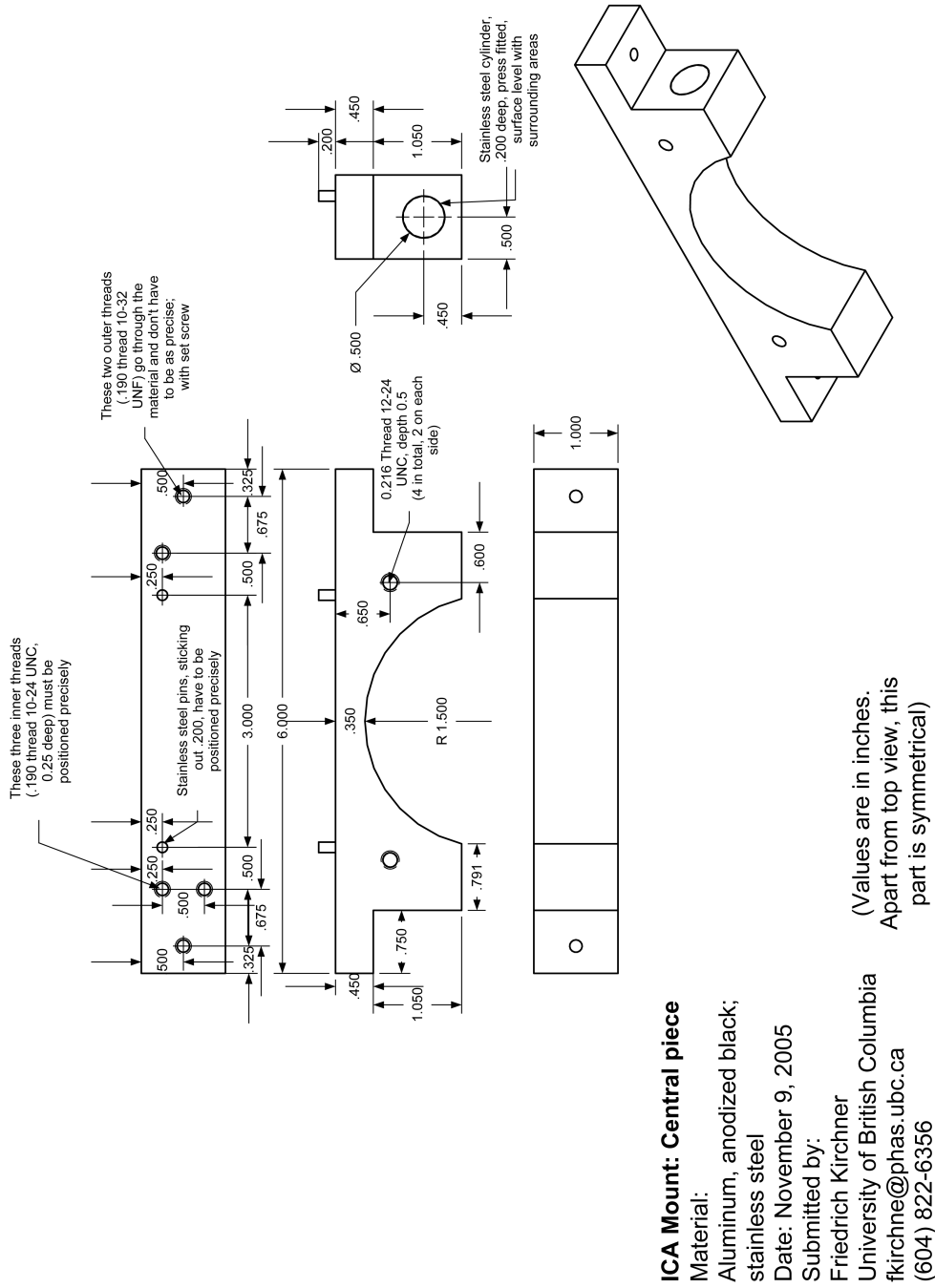


Figure 3: Central piece of ICA mount

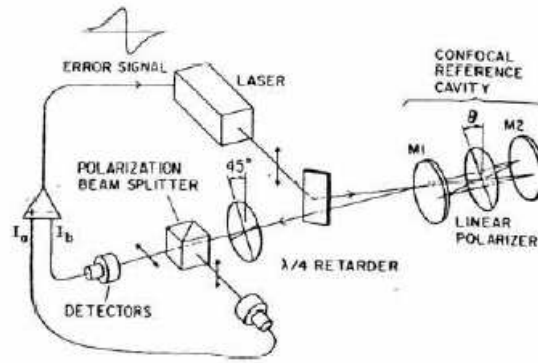


Figure 4: Scheme for laser frequency stabilization (from [1])

However, since we decided to purchase the control box for the laser from Coherent, we had to change our plans in order to secure the compatibility of our reference cavity setup with the control electronics. Therefore, we will now use the locking technique which Coherent uses. This technique will be described after the Hänsch-Couillaud lock.

3.3.1 Hänsch-Couillaud Locking Scheme

The objective of this setup developed by T. W. Hänsch and B. Couillaud [1] is to obtain an error signal which can be used to lock a laser to one of the modes of a stabilized reference cavity.

A schematic drawing of the setup can be found in Figure 4. The locking scheme consists of the following components:

Confocal reference cavity A confocal cavity is used because it causes an off-axis incident ray to retrace itself after traversing the cavity length a total of four times.

Linear polarizer within the reference cavity A polarizer is positioned in the cavity forming an angle θ with the plane of polarization of the laser light.

$\lambda/4$ plate A $\lambda/4$ plate transforms the incident elliptically polarized light into a superposition of orthogonal, linearly polarized waves. The $\lambda/4$ plate is oriented at a 45° angle with respect to the principal axes of the beam splitter.

Polarization beam splitter A polarization beam splitter is used to separate the linearly polarized waves produced by the $\lambda/4$ plate.

Two detectors Two photodiodes allow to measure the intensities of the two components of the light coming from the reference cavity.

3 Upgrade

Light from the laser source shines into the confocal reference cavity at a small angle with the cavity's optical axis so that the reflected beam does not travel back into the laser. A part of the incident light is reflected directly from the input mirror of the resonator. Because of the linear polarizer in the reference cavity, the loss in the cavity depends on the polarization of the incident wave. In the extreme case, when light polarized at 90° with respect to the polarizer shines into the cavity, the loss is 100% because the light cannot pass the polarizer. Therefore, it makes sense to split the incident wave, which is approximated as a plane wave with amplitude $E^{(i)}$, into two components with amplitudes $E_{\parallel}^{(i)} = E^{(i)} \cos \theta$ and $E_{\perp}^{(i)} = E^{(i)} \sin \theta$, which are oriented parallel or perpendicular to the orientation of the polarizer, respectively. As described above, the perpendicular component is not allowed to exist within the cavity. This is why it is completely reflected from the front mirror of the cavity. For the parallel component, however, the cavity has a much lower loss. That is why the parallel component experiences a phase shift when it is reflected from the cavity. The components of the reflected wave are denoted by $E_{\parallel}^{(r)}$ and $E_{\perp}^{(r)}$.

$$E_{\parallel}^{(r)} = E_{\parallel}^{(i)} \left\{ \sqrt{R_1} - \frac{T_1 R}{\sqrt{R_1}} \frac{\cos \delta - R + i \sin \delta}{(1 - R)^2 + 4R \sin^2 \frac{1}{2} \delta} \right\} \quad (1)$$

$$E_{\perp}^{(r)} = E_{\perp}^{(i)} \sqrt{R_1} \quad (2)$$

R_1 and T_1 are the reflectivity and the transmissivity of the cavity entrance mirror M_1 , δ is the phase difference between wave in successive roundtrips ($\delta = 2\pi m$, $m \in \mathbb{N}$, if incident wave is in resonance with the cavity), and $R < 1$ is the amplitude ratio between successive round trips, which includes all losses acquired on one round trip. The opposite sign of the two components in Equation (1) is caused by the fact that one component experiences internal reflection whereas the other is reflected externally. As can be seen from Equation (1), there is no phase shift (imaginary part equals zero), when the incident light is in resonance with the cavity. In this case the reflected light is still linearly polarized. If the incident light is off resonance, the parallel component experiences a phase shift upon reflection, and the total reflected light is elliptically polarized. The orientation of the polarization (right or left-handed) depends on whether the incident wavelength is below or above resonance.

In order to analyze the elliptically polarized light, it is sent through the quarter-wave retarder and the polarization beam splitter. The elliptically polarized light can be described as a superposition of two circularly polarized waves with opposite orientations and different amplitudes. These two components are converted into two perpendicular, linearly polarized waves by the $\lambda/4$ plate. These two waves are separated by the polarization beam splitter and their intensities I_a and I_b are measured with the photodiodes. In case the light coming from the cavity is linearly polarized (laser on resonance with reference cavity), the two circularly polarized waves have equal amplitude. Otherwise, the relative intensities of the

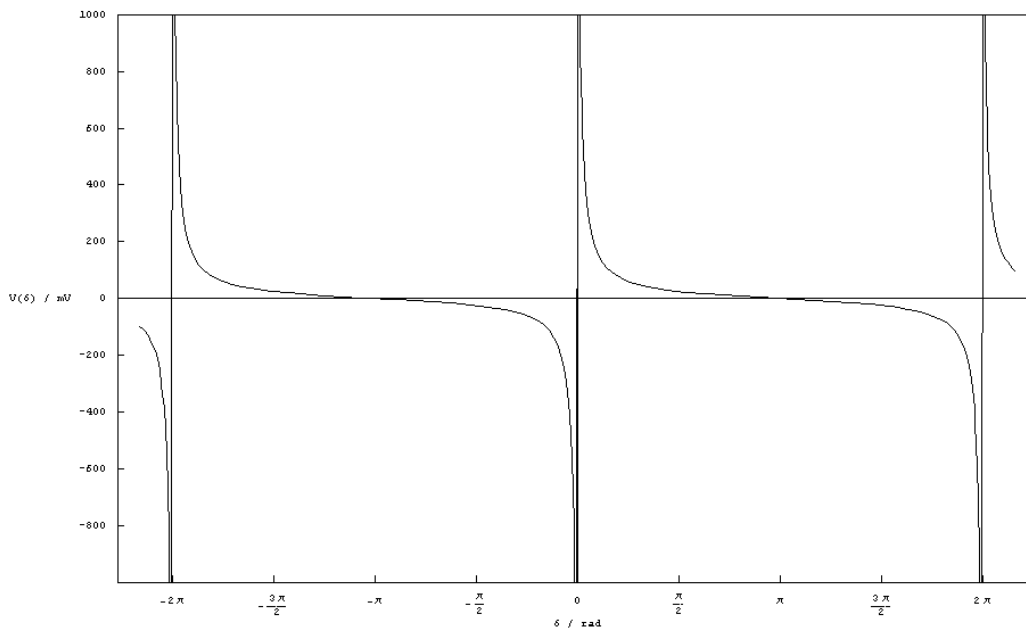


Figure 5: Error signal

two waves will reflect the ellipticity and the orientation of the wave reflected from the cavity.

The output signals of the (calibrated) photodiodes are subtracted in a differential amplifier. Thus the resulting error signal (assuming linear amplification) is proportional to

$$I_a - I_b = I^{(i)} 2 \cos \theta \sin \theta \frac{T_1 R \sin \delta}{(1 - R)^2 + 4R \sin^2 \frac{1}{2} \delta}, \quad (3)$$

where $I^{(i)} = \frac{1}{2} c \epsilon |E^{(i)}|^2$ is the intensity of the incident light. This signal is plotted in Figure 5 for $\theta = 45^\circ$ for some assumed values. It is very suitable as an error signal, because it is relatively strong even at larger distances from the resonance.

3.3.2 Coherent Locking Technique

The Coherent locking setup uses a so-called side lock which works as follows. The optical setup of the Coherent reference cavity can be seen in Figure 6. I will refer to the signals from photodiodes A and B as I_A and I_B , respectively.

A small part of the output from the 899 laser is directed towards the reference cavity (e. g. via a polarization beam splitter). One half of this light passes through the reference cavity

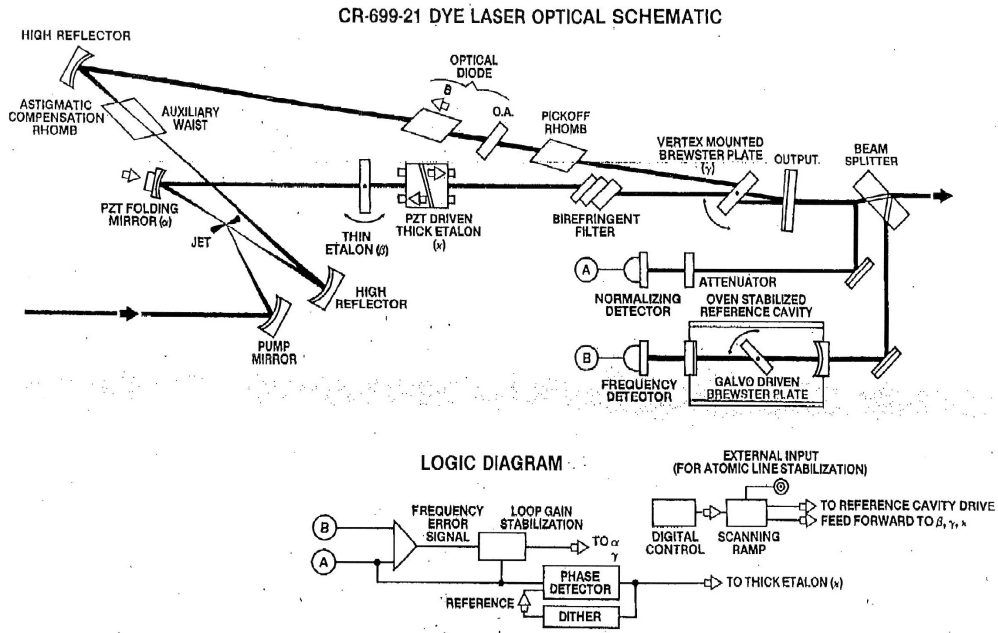


Figure 6: CR-699 dye laser, optical schematic (from [3])

and then hits a photodiode, the other half shines directly onto a second photodiode. The intensities at the two photodiodes must be adjusted so that they produce equal signals when the reference cavity is on resonance.

The signals from the two photodiodes are then processed electronically. The error signal is proportional to $\frac{0.5I_A - I_B}{0.5I_A}$ ($-1 \leq \frac{0.5I_A - I_B}{0.5I_A} \leq 1$). This corresponds to the lock point shown in Figure 7. Depending on sign of the frequency offset, the error signal will be either positive or negative. Thus, it can be used to lock the laser frequency.

3.3.3 Overall Locking Setup

The system will have the following locking scheme. A small part of the light which is emitted from the 899 is analyzed in the stabilized reference cavity, as described above. The signals from the photo diodes is fed into the ICA control box, which will steer the elements of the 899 laser. Thus, the 899 laser will be locked to the reference cavity.

As a second step, parts of the stabilized light from the 899 laser will be mixed with a precisely known reference frequency comb, which consists of equally spaced frequencies spanning a certain bandwidth. This mixing creates several beat notes with frequencies equal to the difference between the laser frequency and each of the comb frequencies.

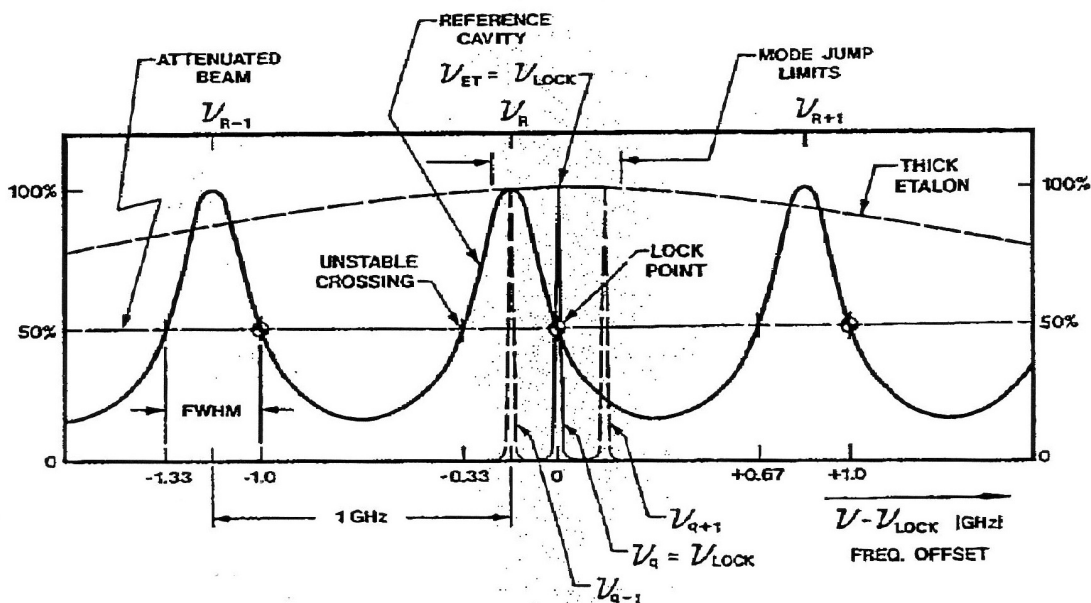


Figure 7: Coherent reference cavity: transmission (from [2])

The beat notes are then low pass filtered (only difference frequency with the closest comb element passes) and measured phase-sensitively with a lock-in amplifier. This creates a second error signal which characterizes the difference of the frequency of the 899 laser from the reference frequency defined by the comb. This error signal can then be used to tune the reference cavity (via the galvo with the brewster plate). The 899 laser will follow as described in the previous paragraph. In the end, the 899 laser will be frequency stabilized to the reference frequency of the comb.

3.4 Reference Cavity

Since we decided to copy the Coherent locking technique, we wanted the characteristics of our reference cavity to match those of Coherent's reference cavity. Fortunately, Coherent provided us with some graphs and diagrams [2] from which I was able to determine the free spectral range ν_f and the finesse \mathcal{F} of the Coherent reference cavity.

From Figure 7, I determined the free spectral range to be $\nu_f = 1$ GHz and the fringe width to be $\delta\nu_{FWHM} = 0.33$ GHz. This results in a finesse $\mathcal{F} \approx 3.17$.

Thus a round trip photon survival probability of $R = 14.83\%$ is required. This determines our choice of mirror reflectivity. The cavity will be a confocal setup with $R = -15$ cm

spherical mirrors. A confocal resonator setup has the advantage of being less sensitive to misalignment of the incident beam, because its resonance frequencies will not change even if we do not couple in a (0,0)-mode beam.

In order to lock this cavity to an external source (i.e. a frequency comb) we will also need a galvo with a Brewster plate within the reference cavity to tune its optical path length.

I also calculated the rotation angle that would be needed for a 100 GHz scan of the cavity (assuming $\nu = 400$ THz). For a Brewster plate of 1 mm thickness, the required angle would be about 7° ($\pm 3.5^\circ$ around Brewster's angle). The effect of the turning Brewster plate on the round trip survival probability of photon is negligible. Thus, the mirror reflectivity should be $R_{Ref} = 38.5\%$.

4 Additional Work

4.1 Lithium Absorption Spectroscopy

When the work on the 899 laser upgrade was on halt because we were waiting for parts to come in, I helped Swati Singh, another master's student in Kirk Madison's lab, with her experiment which can be seen in Figure 8. Her work involves performing absorption spectroscopy with lithium. Swati had constructed a heat pipe in which samples of lithium can be heated in order to increase the lithium vapor pressure. Thus, a strong absorption signal can be achieved.

The heat pipe is constructed such that a laser beam can be directed through the lithium gas. This laser beam is reflected off a mirror and sent back through the heat pipe. The two beams overlap so that saturated absorption measurements can be performed.

The main objective of this work, however, is not to perform this spectroscopy but rather to use the Li D2 ($2^2S_{1/2} - 2^2P_{3/2}$) transition as a reference. Only a small part of the beam from a master laser is sent through the heat pipe, most of it is injected into a slave laser. The slave laser serves as an amplifier emitting about 5 to 10 times the incident intensity at exactly the incident wavelength. The light emitted from the slave laser is amplified again in a broad-area diode laser (BAL). Thus, if the master laser is stabilized to the Li transition mentioned above, the BAL will provide high intensity light at exactly the frequency of that transition. This laser radiation can then be used to laser cool lithium in a magneto-optical trap (MOT).

My work on this experiment included aligning the optical setup so that light shines through the heat pipe, measuring lithium spectra, and injecting the slave laser. Figure 9 shows one of the spectra we measured.

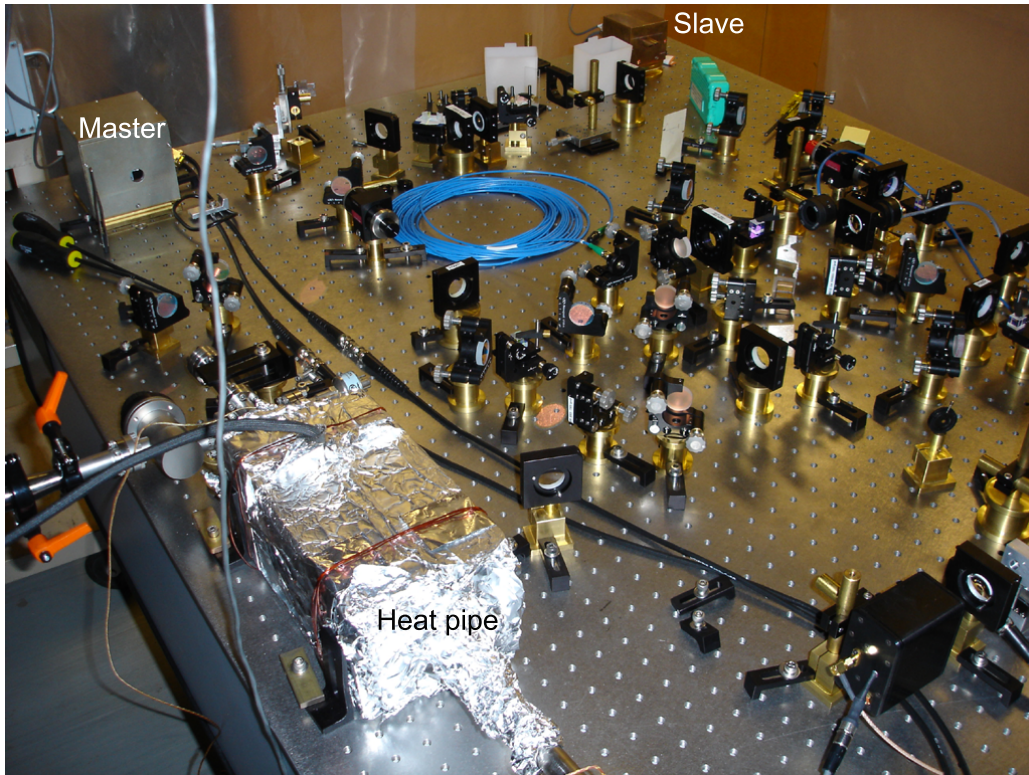


Figure 8: Optical table for Li absorption experiment

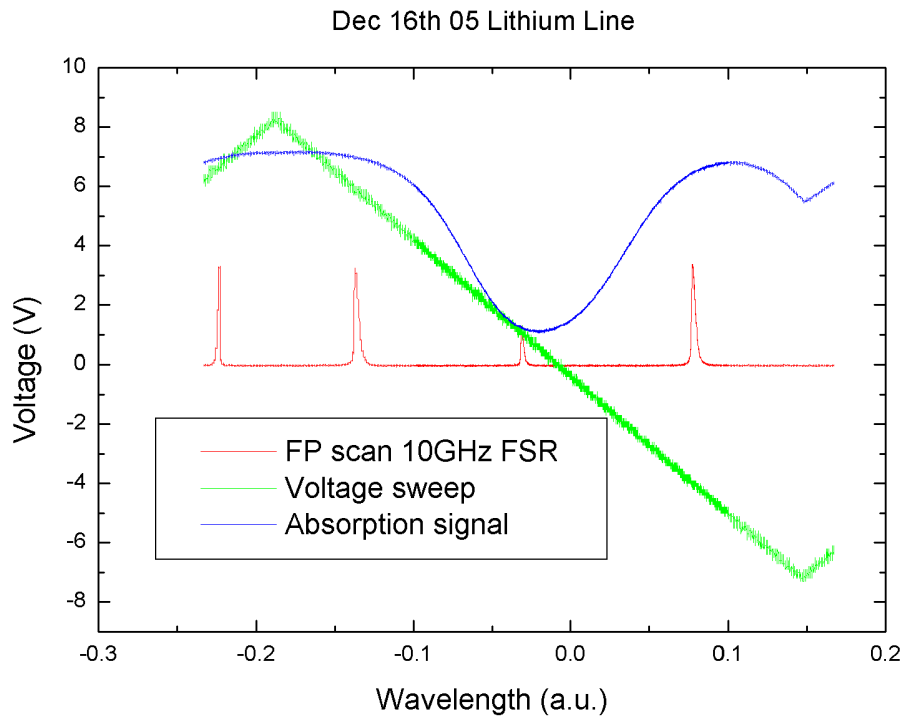


Figure 9: Lithium D2 line absorption and transmission of light through a Fabry-Perot cavity with a 10 GHz free spectral range given for comparison. The voltage ramp for tuning the laser is also shown.

References

- [1] T. W. Hänsch and B. Couillaud: *Laser Frequency Stabilization by Polarization Spectroscopy of a Reflecting Reference Cavity*, Optics Communications, **35**, 441 (1980)
- [2] Coherent: *Figure 1.1-24. Reference Cavity: Transmission*, facsimile
- [3] Coherent: *Figure 1. CR-699 Dye Laser, Optical Schematic*, facsimile